The approximation of the total constant of dissociation as a function of only the translational temperature cannot be extended to a change in flow regimes for motion of bodies along a smooth re-entry trajectory.

NOTATION

T, T_v, translational and vibrational temperatures; K^0, K, equilibrium and total dissociation rate constants; D, energy of dissociation; k, Boltzmann constant; Z, statistical sum of the vibrational levels; θ characteristic temperature of the molecules; T_w, equilibrium temperature of the surface; q, heat flux; t, descent time; H, height; V_∞ flight velocity; y, distance from the body along the normal.

LITERATURE CITED

1. A. G. Tirskii, V. S. Shchelin, and V. G. Shcherbak, Mat. Modelirov., **2**, No. 4, 28-38 (1990).
2. O. É. Krivonosova, S. A. Losev, V. P. Nalivaiko, et al., Khim. Plazmy, No. 14, 3-31 (1987).
3. S. A. Losev and N. A. Generalov, Dokl. Akad. Nauk SSSR, **141**, No. 5, 1072-1075 (1961).
4. P. V. Marrone and C. E. Treanor, Phys. Fluids, **6**, No. 9, 1215-1221 (1963).
5. B. V. Kuksenko and S. A. Losev, Dokl. Akad. Nauk SSSR, **185**, No. 1, 69-72 (1969).
6. K. L. Wray, E. V. Feldman, and P. F. Lewis, J. Chem. Phys., **53**, No. 11, 4131-4136 (1970).
7. C. Park, "Assessment of a two-temperature kinetic model for dissociating and weakly-ionizing nitrogen," AIAA paper No. 1347, New York, (1986).
8. G. E. Lozino-Lozinskii, The Gagarin Scientific Lecture Series on Cosmonautics and Aviation 1989 [in Russian], Moscow (1990), pp. 6-21.

INFLUENCE OF THERMAL EFFECTS ON THE PROCESS OF HIGH-VELOCITY PENETRATION OF A FLUORO-POLYMER PLATE

V. A. Gorel'skii and S. A. Zelepugin

UDC 539.537

We examine the problem of high-velocity impact of a steel cylinder on a fluoro-polymer plate. The finite-element numerical method is used to study the distributions of thermal and mechanical variables which result from the process of this axisymmetric interaction. The features of plate penetration are revealed when the temperature in some regions of the fluoro-polymer exceed melt, and thermal dissociation takes place.

Introduction. The broad application of polymer materials in technology has made the study of their behavior under extreme conditions, particularly under shock-wave loading, topical [1]. Certain aspects of the behavior of polymers under high-velocity impact conditions have already been reflected in the experimental works of [2, 3], where the effects of heating on the strength properties of polymers was shown.

However, numerical calculations are needed to determine the dynamics of the temperature field distribution which arises in the penetration process, and to evaluate the influence of this field on the mechanical characteristics of the material. The goal

Institute of Structural Macrokinetics, Tomsk Branch, Russian Academy of Sciences, Tomsk.

Translated from Inzhenerno-Fizicheskii Zhurnal, Vol. 62, No. 4, pp. 564-568, April, 1992. Original article submitted August 2, 1991.

1062-0125/92/6204-0406$12.50

of our work is to study numerically the process of penetration of a teflon plate by a steel projectile. The calculations were done using the finite-element method within the limits of a model of an elastic–plastic medium which can sustain damage. Additional complications in the calculations arise because the temperature in certain regions of the fluoro-polymer exceed melt in the range of interaction conditions being studied here, which results in significant changes in the material characteristics.

Mathematical Model. The system of equations describing the unsteady adiabatic motion of a compressible medium, and which accounts for changing porosity, and has axial symmetry, consists of the equations of continuity, motion, energy, and change in the specific pore volume [4]:

$$\dot{\rho} = -\rho(v_{,z} + u_{,r} + u/r), \tag{1}$$

$$\rho\dot{u} = s_{rr,r} + s_{rz,z} + (s_{rr} - s_{\theta\theta})/r - p_{,r}, \tag{2}$$

$$\rho\dot{v} = s_{rz,r} + s_{zz,z} + s_{rz}/r - p_{,z}, \tag{3}$$

$$\rho\dot{E} = p\dot{\rho}/\rho + s_{zz}v_{,z} + s_{rr}u_{,r} + s_{\theta\theta}u/r + s_{rz}(u_{,z} + v_{,r}), \tag{4}$$

$$\begin{gathered} \dot{V}_p = 0 \text{ for } |p_c| \leqslant p_k V_1/(V_p + V_1) \text{ or } (p_c > p_k V_1/(V_p + V_1) \text{ and } V_p = 0), \\ \dot{V}_p = -\operatorname{sign}(p_c)\, k_4\,[|p_c| - p_k V_1/(V_p + V_1)]\,(V_p + V_2) \\ \text{for } p_c < -p_k V_1/(V_p + V_1) \text{ or } (p_c > p_k V_1/(V_p + V_1),\ V_p > 0). \end{gathered} \tag{5}$$

According to [4,5], the pressure in the continuous component of the material is a function of the specific volume, internal energy, and the specific pore volume:

$$\begin{gathered} p_c = \rho_0 a^2 \mu + \rho_0 a^2 [1 - \gamma_0/2 + 2(b-1)]\mu^2 + \\ + \rho_0 a^2 [2(1 - \gamma_0/2)(b-1) + 3(b-1)^2]\mu^3 + \gamma_0 \rho E, \end{gathered} \tag{6}$$

where $\mu = V_0/(V - V_p) - 1$; a, b are material constants from known relations, which relate the velocity of the shock front D with the material velocity of the shock-compressed material u_m [6]: $D = a + bu_m$. The average pressure in the medium in the presence of pores is determined from the relation $p = p_c\rho/\rho_c$. The stress deviator components are found from

$$\begin{gathered} 2G\left(v_{,z} + \frac{1}{3}\frac{\dot{\rho}}{\rho}\right) = s_{zz}^{\nabla} + \lambda s_{zz},\quad 2G\left(u_{,r} + \frac{1}{3}\frac{\dot{\rho}}{\rho}\right) = s_{rr}^{\nabla} + \lambda s_{rr}, \\ 2G\left(u/r + \frac{1}{3}\frac{\dot{\rho}}{\rho}\right) = s_{\theta\theta}^{\nabla} + \lambda s_{\theta\theta},\quad G(u_{,z} + v_{,r}) = s_{rz}^{\nabla} + \lambda s_{rz}. \end{gathered} \tag{7}$$

The index ∇ denotes the Jaumann derivative. The parameter $\lambda = 0$ for elastic strains, while for plastic strains ($\lambda \geq 0$), it is determined with the help of the von Mises yield condition

$$s_1^2 + s_2^2 + s_3^2 = \frac{2}{3}\sigma^2. \quad (8)$$

The shear modulus and the yield limit are determined according to

$$\begin{gathered} G = G_0 [1 + cp/(1+\mu)^{1/3} + h(T-300)] V_3/(V_p + V_3), \\ \sigma = \sigma_0 [1 + cp/(1+\mu)^{1/3} + h(T-300)](1 - V_p/V_4), \\ G = 0, \ \sigma = 0, \quad \text{if } T > T_m, \ \sigma = 0, \quad \text{if } V_p > V_4. \end{gathered} \quad (9)$$

The temperature is computed according to the formula given in [6]:

$$\begin{gathered} T = (E - E_{0x})/c_p = [E - E_0 - E_1\mu - (-E_1 + E_2)\mu^2 - \\ -(E_1 - 2E_2 + E_3)\mu^3 - (-E_1 + 3E_2 - 3E_3 + E_4)\mu^4]/c_p. \end{gathered} \quad (10)$$

The constants in (10) have the form

$$\begin{gathered} E_0 = -300c_p, \ E_1 = \gamma_0 E_0, \ E_2 = (a^2 + \gamma_0^2 E_0)/2, \\ E_3 = (4ba^2 + \gamma_0^3 E_0)/6, \ E_4 = (-2\gamma_0 ba^2 + 18b^2a^2 + \gamma_0^4 E_0)/24. \end{gathered}$$

When the melt temperature is reached, (10) is modified in such a way that the temperature remains constant until the end of the material melting process. During melting of the material, which is accompanied by a loss of strength, we use a material model in the calculations which corresponds to that described in [7] for a viscous compressible material, since in our work, the stress deviators include viscous components $s_{ij}^V = 2\mu^V \varepsilon_{ij}$ [8]. The numerical value of the coefficient of viscosity μ^V is determined from values given in [9].

We consider the problem of the interaction of a steel cylindrical projectile, occupying region D_1, with a fluoro-polymer plate occupying region D_2. For (1)-(10), we pose the problem with initial conditions at t = 0 and boundary values given at the surfaces. The initial conditions have the form:

$$\begin{gathered} s_{rr}(0, r, z) = s_{zz}(0, r, z) = s_{\theta\theta}(0, r, z) = s_{rz}(0, r, z) = p(0, r, z) = \\ = E(0, r, z) = V_p(0, r, z) = 0 \ ((r, z) \in D_1 \cup D_2), \ v(0, r, z) = v_0 \ ((r, z) \in D_1), \\ v(0, r, z) = 0 \ ((r, z) \in D_2), \ u(0, r, z) = 0 \ ((r, z) \in D_1 \cup D_2), \\ \rho(0, r, z) = \rho_1 \ ((r, z) \in D_1), \ \rho(0, r, z) = \rho_2 \ ((r, z) \in D_2). \end{gathered}$$

At the free surfaces, the following conditions hold: $T_{NN} = T_{N\tau} = 0$; and at the contact surface between the projectile and the plate the following slip conditions are used: $T_{NN}^+ = T_{NN}^-$, $T_{N\tau}^+ = T_{N\tau}^- = 0$, $v_N^+ = v_N^-$. Here N is a unit vector normal to the surface at the point under consideration; τ is a unit vector tangent to the surface at this point; T_N is the vector force on the area with nromal N; v is the vector velocity. The subscripts on the vectors T_N and v denote the projection onto the corresponding vector bases. The superscript plus characterizes variable values in the material at the upper boundary of the contact surface, the superscript minus, those at the lower boundary.

To solve this problem, we use the finite-element method presented in [10, 11].

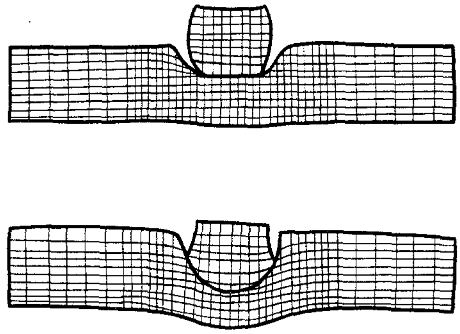

Fig. 1. Snapshots of the interaction process at 2.5 and 5 μsec.

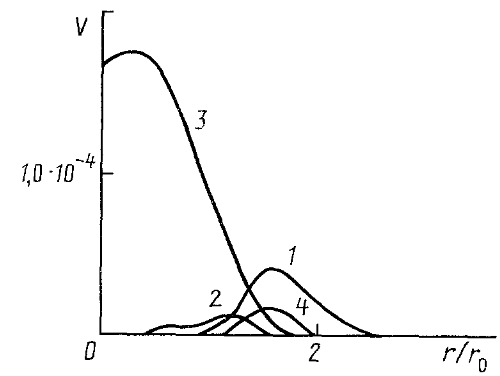

Fig. 2. Distribution of specific pore volume in representative radial cross-sections of the plate: 1) front surface, 5 μsec after impact; 2) middle of the plate, after 5 μsec; 3) rear surface, after 5 μsec; 4) front surface, after 2.5 μsec. V, m^3/kg.

Numerical Results. We numerically modelled a cylindrical steel projectile of diameter 5 mm and length 5 mm interacting with a teflon plate of thickness 5 mm. The impact velocity was 1000 m/sec. In the calculations, the behavior of the teflon was characterized by the following parameters [12, 13]: $\rho_0 = 2200$ kg/m^3, $a = 1680$ m/sec, b = 1.82, $\gamma_0 = 2.64$, $G_0 = 0.234$ GPa, h = -0.015 K^{-1}, c = 0, $\sigma_0 = 0.012$ GPa, $V_1 = 4.6 \cdot 10^{-5}$ m^3/kg, $V_2 = 2.27 \cdot 10^{-7}$ m^3/kg, $V_3 = 4.55 \cdot 10^{-4}$ m^3/kg, $V_4 = 1.818 \cdot 10^{-3}$ m^3/kg, $k_4 = 0.03$ m·sec/kg, $p_k = -0.024$ GPa, $c_p = 1.05$ kJ/(kg·K), $T_m = 600$ K, $\Delta H_m = 62.1$ kJ/kg. The projectile material was steel, characterized by the following parameters: $\rho_0 = 7850$ kg/m^3, $a = 4415$ m/sec, b = 1.553, $\gamma_0 = 1.91$, $G_0 = 79$ GPa, h = $1.6 \cdot 10^{-4}$, K^{-1}, c = 206.0 GPa^{-1}, $\sigma_0 = 0.87$ GPa, $V_1 = 0.26 \cdot 10^{-5}$ m^3/kg, $V_2 = 0.89 \cdot 10^{-6}$ m^3/kg, $V_3 = 2.55 \cdot 10^{-5}$ m^3/kg, $V_4 = 7.64 \cdot 10^{-5}$ m^3/kg, $k_4 = 0.52$ m·sec/kg, $p_k = -1.5$ GPa, $c_p = 446.7$ J/(kg·K).

Figure 1 shows numerical snapshots corresponding to times 2.5 and 5 μsec of the interaction of the projectile with the fluoro-polymer plate. The calculations indicate that for an impact velocity of 1000 m/sec, the plate is penetrated, and although the projectile remains intact, it is significantly deformed. The features of plate failure are illustrated in Fig. 2, which shows the dynamics of pore development in the fluoro-polymer at representative surfaces of the plate. Analysis of the plots indicates that the penetration of the plate takes place as a result of a plugged-out disk, whose diameter on the front surface is approximately 1.8 times larger than the initial diameter of the projectile. With decreasing distance from the back surface, the diameter of the excised disk decreases, and its final separation takes place as a result of tensile stresses acting in the radial direction. The evolution of the temperature field in the fluoro-polymer is shown in Fig. 3. It is obvious from this figure that under conditions of high velocity impact, a temperature field with large gradients is formed in the plate in the zone of intense

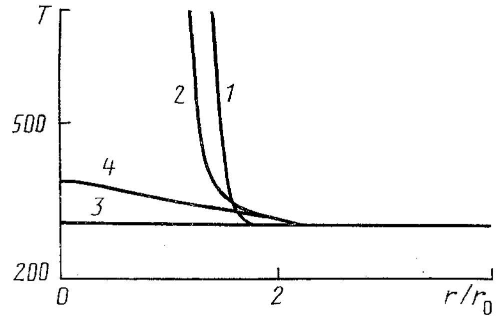

Fig. 3. Temperature distribution in representative radial cross-sections of the plate: 1) front surface, 5 μsec after impact; 2) middle of the plate, after 5 μsec; 3) rear surface, after 5 μsec; 4) middle of the plate, after 2.5 μsec. T, K.

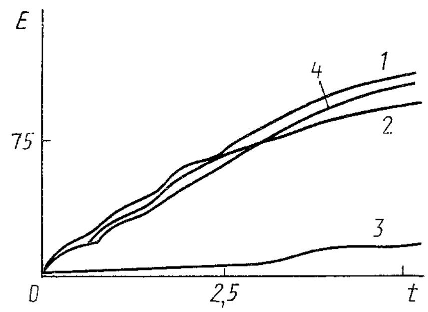

Fig. 4. Time dependences characterizing changes in the integral energy variables of the interacting bodies: 1) internal energy of the plate; 2) internal energy of the projectile; 3) kinetic energy of the plate; 4) shear strain energy of the plate. E, kJ; t, μsec.

shear deformations. As a result of this, by 5 μsec, a significant portion of the plate material which is in contact with the projectile is in a state of thermal dissociation. On the other hand, at both the back surface and beyond the limits of the heated disk which is being plugged out, the values of the temperature remain close to their initial values. The dynamics of the penetration process as a whole make it possible to plot the integrated energy parameters of the impacting bodies as a function of time (Fig. 4). From the calculations, it follows that during the interaction, the kinetic energy of the projectile is for the most part converted into internal energy in the plate, and, to a somewhat lesser degree, into internal energy of the projectile itself. The plots show that in the first 2.5 μsec, the process has a pronounced wave-like character; subsequently, all curves become more monotonic. The kinetic energy acquired in the impact process constitutes an insignificant fraction of the total energy balance.

CONCLUSION

Thus, the results of our study indicate that intense heating in the upper part of the fluoro-polymer plate in the high-velocity impact regime leads to melting and thermal destruction in this region of the plate. Mechanical failure of the fluoro-polymer takes place in the lower part of the plate, but the region undergoing failure occupies a relatively small volume of material.

NOTATION

ρ, density; u, v, radial and axial components of the vector velocity; r, Θ, z, axes of the cylindrical coordinate system (z is the axis of symmetry); s_{rr}, s_{zz}, $s_{\theta\theta}$, s_{rz}, components of the stress deviator tensor; p, average pressure; p_c, pressure in the continuous component of the material; E, specific internal energy; V_p, specific pore volume; V_0 and V, initial and current values of the specific volume; γ_0, Gruneisen ratio; T, temperature; E_{0x}, cold component of the specific internal energy; c_p, specific heat capacity; G, shear modulus; σ, yield limit; $s_{1,2,3}$, principal components of the stress deviator tensor; T_m, melt temperature; t, time; $V_{1,2,3,4}$, k_4, p_k, ρ_0, a, b, G_0, σ_0, c, h, material constants. A dot over a variable denotes the time derivative; v_z denotes the derivative with respect to the coordinate.

LITERATURE CITED

1. K. B. Baknell, The Impact Strength of Plastics [Russian translation], Leningrad (1981).
2. V. P. Muzychenko and V. I. Postnov, Probl. Prochn., No. 8, 62-66 (1986).
3. V. K. Golubev and S. A. Novikov, Zh. Prikl. Mekh. Tekh. Fiz., No. 6, 140-145 (1987).
4. V. A. Gorel'skii, A. V. Radchenko, and I. E. Khorev, Izv. Akad. Nauk SSSR, Mekh. Tverd. Tela, No. 6, 185-189 (1988).
5. L. Seaman, D. R. Curran, and D. A. Shockey, J. Appl. Phys., **47**, No. 11, 4814-4826 (1976).
6. W. H. Gust, J. Appl. Phys., **53**, No. 5, 3566-3575 (1982).
7. L. M. Stel'makh, A. M. Stolin, and B. M. Khusid, Inzh.-Fiz. Zh., **61**, No. 2, 268-276 (1991).
8. I. E. Khorev, and V. A. Gorel'skii, Detonation. Material from the Second All-Union Conference on Detonation [in Russian], Vol. 2, Chernogolovka (1981), pp. 149-153.
9. Z. Tadmor and K. Goros, Theoretical Foundations of Polymer Processing [Russian translation], Moscow (1984).
10. G. R. Johnson, J. Appl. Mech., **43**, No. 3, 439-444 (1976).
11. V. A. Gorel'skii, I. E. Khorev, and N. T. Yugov, Zh. Prikl. Mekh. Tekh. Fiz., No. 4, 112-118 (1985).
12. Yu. A. Panshin, S. G. Malkevich, and Ts. S. Dunaevskaya, Fluoro-plastics [in Russian], Leningrad (1978).
13. V. A. Gorel'skii and S. A. Zelepugin, Rheology and Thermal Physics of Non-Equilibrium Systems. Material from the International School-Seminars. Volume 2: Kinetic Processes in Condensed Media [in Russian], Minsk (1991), pp. 110-113.